Carsharing with fuel cell vehicles: Sizing hydrogen refueling stations based on refueling behavior

Fabian Grüger[a], [*], Lucy Dylewski[b], Martin Robinius[c], Detlef Stolten[c, d]

[a] *Reiner Lemoine Institut gGmbH, Rudower Chaussee 12, 12489 Berlin, Germany*
[b] *Civity Management Consultants GmbH & Co. KG, Tesdorpfstr. 11, 20148 Hamburg, Germany*
[c] *Institute of Electrochemical Process Engineering (IEK-3), Forschungszentrum Jülich GmbH, Wilhelm-Johnen-Str., D-52428, Germany*
[d] *Chair for Fuel Cells, RWTH Aachen University, c/o Institute of Electrochemical Process Engineering (IEK-3), Forschungszentrum Jülich GmbH, Wilhelm-Johnen-Str., D-52428, Germany*

ABSTRACT

Fuel cell vehicles and carsharing depict two potential solutions with regard to pollution and noise from traffic in cities. They are most effective when combined, and hydrogen is produced via electrolysis using renewables. One major hurdle in utilizing fuel cell vehicles is to size hydrogen refueling stations (HRS) and hydrogen production via electrolysis properly in order to fulfill the carsharing vehicles' demand at any given time. This paper presents data on refueling behavior in free-floating carsharing, which have not been available thus far. Refueling profiles of hydrogen carsharing vehicles are modeled based on this data. Furthermore, this analysis presents and applies a methodology for optimizing topology of a wind turbine-connected HRS with onsite electrolysis via an evolutionary algorithm. This optimization is conducted for different carsharing fleet sizes, and HRS profitability is evaluated. The results show that larger fleets are capable of decreasing hydrogen production costs significantly. Moreover, adding capacity to the HRS in order to prepare for hydrogen demand from private vehicles in the future does not significantly increase costs. However, overall costs are still high compared to the current market price in Germany, requiring further cost reductions.

1. Introduction

Currently, transportation accounts for a significant share in CO_2 emissions worldwide as well as in Germany [1,2]. Additionally, cities are struggling with high air pollution due to vehicle tailpipe emissions, leading to discussions about banning vehicles, especially diesel cars, from inner cities. Thus, in order to maintain personal mobility and regain a higher air quality in cities, a transportation transition is required. According to Agora Verkehrswende [3], this transition can be perceived as change in mobility behavior on the one hand and energy transition in the transportation sector on the other hand. One approach of providing mobility more efficiently is carsharing, which can reduce the number of cars on the road if substituting privately owned cars. In contrast, energy transition in transportation requires vehicle concepts capable of using renewables as an energy source. One of the most promising options in this regard are fuel cell electric vehicles (FCEV) fueled by hydrogen. Thus, especially the combination of both approaches, carsharing and FCEV, might become an important means in

order to deal with the aforementioned problems. This approach already has been applied in recently emerged projects in major cities in Germany (see literature review in Section 2.1). But hydrogen refueling infrastructure is scarce and needs to be complemented if carsharing vehicles demand hydrogen at a larger scale. This raises the question of how hydrogen refueling stations (HRS) for carsharing should be designed in terms of hydrogen production and storage capacity, and which costs these stations are associated with. Therefore, this study presents data on refueling behavior of free-floating carsharing vehicles in six German cities collected over a period of seven months. Based on these data, this paper provides a novel and comprehensive approach of sizing hydrogen refueling stations with onsite electrolysis. It is applied to a case of combined hydrogen demand of private and carsharing vehicles and optimizes hydrogen production costs.

The remaining part of this section gives an overview of carsharing and hydrogen as a fuel, while Section 2 provides a literature review. Sections 3 and 4 describe the methodology and the investigated scenar-

---
[*] Corresponding author.
Email address: fabian.grueger@rl-institut.de (F. Grüger)

ios, respectively. Results are presented and discussed in Section 5, followed by conclusions in Section 6.

1.1. Carsharing

The concept of carsharing allows people to use one car or a pool of cars collectively in a sequential manner. Thus, taking part in carsharing might make owning a car unnecessary. This can lead to lower mobility costs for carsharing users, especially if access to a vehicle is not required regularly. Additionally, carsharing is also beneficial to the respective city and the environment since congestion can be reduced, and people are encouraged to use public transportation more often if they do not own a private car. There are different forms of carsharing: private carsharing, station-based carsharing and free-floating carsharing. Private carsharing is organized by the users themselves, for example, when two neighbors share one vehicle. In contrast, station based and free-floating carsharing are commercial services provided by a company. In most cases, users have to register to the service and can book cars online. They are either charged by distance traveled or by duration of driving. Vehicles of station-based carsharing are parked at selected, designated spots and have to be returned to these spots after usage. Free-floating carsharing, on the other hand, does not require the use of discrete spots for fetching and parking a vehicle. Instead an area of operation within a city is specified. Customers are allowed to park carsharing vehicles wherever they want within this area, so in general, cars are spread out among this area. According to [4], more than 2 million drivers were registered to a carsharing service in Germany by 01.01.2018, which is an increase of 23% compared to the number of registered users by 01.01.2017. These people share nearly 18,000 carsharing vehicles and account for 3.3% of all people holding a driver's license [5].

1.2. Hydrogen as a fuel

FCEV are electric vehicles using pressurized, gaseous hydrogen as an energy carrier. Hydrogen and oxygen are converted onboard into water vapor and electric energy, propelling an electric motor. Thus, instead of harmful tailpipe emissions, there are potential indirect emissions during hydrogen production. In fact, today most HRS rely on delivered hydrogen originating mostly from fossil fuels for cost reasons. In order to achieve a significant reduction of CO_2 emissions, it is therefore important to produce hydrogen via electrolysis using electricity from renewable energy sources. Especially in the initial phase of low market penetration of FCEVs, it can be favorable to utilize electrolysis onsite HRS and avoid central scaled-up hydrogen production and delivery by truck [6]. In other scenarios with a higher overall hydrogen demand, other options like central electrolysis and delivery might become favorable. Besides onsite electrolysis, HRS consist of hydrogen storage tanks at low (~45 bar) and high (~1000 bar) pressure, a hydrogen compressor, and a dispenser including a hydrogen pre-cooler. Using additional cascades of storage tanks can be advantageous in terms of energy consumption [7]. Another established method of storing hydrogen is in liquid form, which requires liquefaction in the first place [8]. In the future, hydrogen storage based on liquid organic hydrogen carriers might be an additional option [9,10]. In Germany, there are to date less than 40 HRS, but the network is growing continuously. Currently, 48 additional stations are under construction, contributing to the target of 100 HRS by 2019 [11]. Due to the low number of FCEV currently on the road, HRS in general suffer from underutilization and cannot be operated profitably. FCEV fleets, like taxis or carsharing fleets, can increase utilization and profitability of HRS, but require additional capacity if deployed in larger numbers. Hydrogen production can be adapted to energy provision from renewables and thus be a

means of flexibility to the overall energy system [12,13,1,14–17]. This flexibility can be especially valuable, when harnessing surplus energy from wind farms [18–20]. Moreover, large scale energy storage can be accomplished at lower costs when using hydrogen storage systems compared to electrical energy based storage systems [21]. Hydrogen is also discussed as a flexible energy carrier for micro grids, used for stationary or mobile applications as well as for storage purposes [22–25].

2. Literature review

The following literature review focuses on the main aspects of this paper: hydrogen based carsharing (Section 2.1), driving and refueling patterns of carsharing drivers in general (Section 2.2), and hydrogen refueling stations (Section 2.3). This chapter concludes with the main contributions of this paper as they contrast with the previously analyzed literature (Section 2.4).

2.1. H2-Carsharing

Literature on hydrogen based carsharing is sparse. Kriston et al. [26] analyzed carsharing with FCEV in Budapest, Hungary in terms of economy. They investigated fleet sizes between 20 and 200 microcars. The investigation focused on business models, and neither the refueling process nor refueling behavior were taken into account. Furthermore, HRS were not part of the analysis.

In fact, there are already two carsharing services in Germany that make use of FCEV in their fleet: BeeZero and CleverShuttle. BeeZero is located in Munich and is a mixture of station-based and free-floating carsharing service. Vehicles are distributed across the city, which is divided into several zones. Customers are required to return the vehicle in the respective zone in which they rented it. The vehicle fleet consists of 50 FCEV [27].

CleverShuttle, by contrast, is a German ridesharing service, so actually it is not a conventional carsharing service. Customers can order a vehicle as they would order a taxi, and additional customers with similar destinations can join the ride en route. Thus, rates are lower than conventional taxi fees. Recently, CleverShuttle integrated 20 FCEV in their fleet in Hamburg [28] and 10 FCEV in Stuttgart [29].

2.2. Driving and refueling patterns

Schmöller et al. [30] analyzed free-floating carsharing operation with conventional vehicles in Munich, Germany. They evaluated hourly data on booking profiles between November 2011 and October 2013. While this provides insights into temporal mobility demand, neither hydrogen as a fuel nor refueling patterns were investigated.

In contrast, Lopes et al. [31] focused on station-based carsharing. Driving patterns are approximated via agent-based simulation. Their model combines survey data on mobility behavior in Lisbon, Portugal with stochastic methods in order to vary temporal trip probability. Refueling was assumed to be taken care of by the carsharing operator, and refueling patterns were not discussed. Moreover, their approximated results do not match the findings of [30].

The study "Urban mobility in Transition" [32] examined changes in urban mobility markets that are based on the example of free-floating carsharing systems. Over 115 million data records were collected to map around 18 million car rentals. The focus was on the evaluation of the relevance of these systems for transport and the economy and the development of recommendations for urban and transport planning, for mobility providers and free-floating carsharing providers. Therefore, driving patterns were evaluated, but refueling patterns were not part of the analysis.

2.3. Hydrogen refueling stations

Literature provides several studies on HRS operation with onsite electrolysis and integration of renewable energy sources. But only few contributions deal with topology optimization of HRS. The following gives an overview of recent analyses in the respective field.

Troncoso et al. [33] developed an optimization tool for sizing an off-grid HRS for aerospace applications. Energy is provided by a high concentrated PV array and hydrogen is produced onsite via electrolysis. However, the system in regard has a low hydrogen production rate and therefore is not applicable to HRS for road vehicles.

Nistor et al. [34] evaluated an HRS with onsite electrolysis and wind farm connection via detailed simulation. Their model comprises cost assumptions both for PEM and alkaline electrolysis. The focus of this study is on operation of a given HRS configuration. Results indicate that relying solely on wind farm connection in terms of energy supply leads to relatively low equivalent full load hours of the electrolyzer while some hydrogen demand remains unfulfilled. However, this analysis does not conduct topology optimization of HRS.

Carr et al. [35] investigated HRS operation with wind farm integration and electricity market participation. An optimization routine was applied to an existing refueling station in Rotherham, UK. Their HRS model is linear and uses half hourly time steps. However, topology optimization was not part of this analysis.

An HRS with wind farm or photovoltaic power plant connection and onsite electrolysis was investigated by Zhao et al. [36]. Additionally, a fuel cell for reconversion of hydrogen into electricity was integrated. Different, rather simple operating strategies were evaluated based on a hydrogen demand profile of an existing HRS in California. The authors also conducted a basic topology optimization by varying the wind farm's and PV's rate power and capacity factor, respectively. Furthermore, they estimated suitable electrolyzer and storage tank dimensioning, but the analysis lacks an optimization of the HRS's components. Moreover, the underlying demand profile does not reflect realistic future hydrogen demand but an early stage situation with only few cars and HRS.

García Clúa et al. [37] analyzed a wind-hydrogen system with electricity grid connection in terms of operating strategies. The focus is on power electronics, and hydrogen demand is neglected. HRS are not taken into account, and topology optimization is not conducted.

Grüger et al. [38] investigated the combination of a wind farm and an electrolyzer via simulation. Two different operation modes were taken into account: The electrolyzer was used for wind farm forecast error compensation in the first mode and for secondary control reserve market participation in the second mode. Hydrogen production costs were calculated but neither further HRS components nor taxes and surcharges were taken into account. Several scenarios differing in the electrolyzer's rated power were simulated but no topology optimization was conducted.

Grüger et al. [39] developed a predictive operating strategy for HRS with onsite electrolysis and wind farm connection under electricity spot market participation. All relevant HRS components were taken into account, and a detailed economic analysis was conducted. The model was based on a realistic hydrogen demand profile with an average daily demand of 168 kg. Results showed that predictive operation is capable of reducing hydrogen production costs. They also compared this setup to an HRS without wind farm connection and found that under current German legislation, wind farm connection is favorable in terms of hydrogen production costs. However, the assumed hydrogen demand does not reflect the current situation of underutilization of HRS, and a topology optimization was not conducted.

HRS and hydrogen production cost sensitivity in the US was investigated by Reddi et al. [40]. The analysis included gaseous as well as liquid hydrogen delivery and respective HRS technology. Results showed that underutilization of HRS in early stages of FCEV deployment leads to high hydrogen production costs.

Li et al. [41] presented a methodology for sizing microgrids via an evolutionary algorithm in combination with a unit commitment strategy. The approach was applied to a system supplying residential electrical load and comprising PV, a battery storage system, an electrolyzer, a fuel cell and hydrogen storage tanks. While the approach could be applied to HRS, such scenarios were not taken into account.

2.4. Main contributions of this paper

This paper presents data on refueling behavior in free-floating carsharing with conventional vehicles. To date, such data are not available though they are necessary in order to investigate carsharing as a sustainable mobility concept, which might become even more important in the future. Refueling behavior of hydrogen carsharing vehicles is modeled based on this data, and HRS demand profiles are derived. Furthermore, this paper presents and applies a methodology for optimizing topology of a wind turbine-connected HRS, i.e. its components' sizes, with the help of an evolutionary algorithm. Although topology optimization of energy systems is not a novelty, it has never been applied comprehensively to an HRS. This optimization is conducted for different carsharing fleet sizes, and HRS profitability is evaluated.

3. Methodology

In this section, the developed and applied methodology is described. Refueling behavior is modelled and demand profiles derived from carsharing (Section 3.1) and private vehicles (Section 3.2). In Section 3.3, the methodology for optimizing HRS topology is explained.

3.1. Modeling refueling behavior and deriving demand profiles from carsharing vehicles

In this analysis, refueling behavior is defined by the relative frequency (or probability), refuelling events take place at a given hour of the week. For this analysis, data on position, vehicle identification number, license plate number, and tank level of free-floating carsharing vehicles are collected. This is achieved by continuously monitoring the websites of two carsharing providers: DriveNow and car2go. Whenever a vehicle is available, it is listed on the respective website. Thus, vehicle data before and after a trip can be extracted. Data were gathered and analyzed from 09.08.2016 until 15.03.2017 for six German cities (Berlin, Cologne, Düsseldorf, Hamburg, Frankfurt, and Munich) and comprise more than 7000 vehicles (the exact number differs slightly among different months). The data are stored every 15 min. Only vehicles with an internal combustion engine are selected for evaluation. Trip data considered are limited to trips showing a higher tank level afterwards than prior to the trip, because at least one refueling event took place in the course of these trips. It is possible that not all refueling events are captured by applying this procedure, because after longer trips the tank level can be lower than at the beginning despite a possible refueling event during the trip. It is assumed, though, that the error due to neglecting such cases is very small and more importantly does not influence the validity of the modelled refueling behavior significantly. Since it is not possible to determine the exact time of refueling from the collected data, the refueling event is estimated to take place in the midst of the trip. The respective tank level at the beginning of refueling is assumed to be the most recent known tank level, i.e. at the beginning of the trip. In addition to trip data, fleet sizes are recorded for each city, month, and provider based on the number of

available vehicles. Since the vehicle identification number and license plate number are stored in the database, vehicles can be distinguished and counted.

These data are used for modeling the refueling behavior and to derive demand profiles for carsharing vehicles. This requires determining the annual mileage, which is not directly available. It can be approximated in three steps, assuming a fleet comprising BMW 1 series (gasoline and diesel, 12.5% each), Mini (gasoline and diesel, 12.5% each) and Smart fortwo (gasoline, 50%). First, the average vehicle range r is estimated by dividing fuel tank volume by fuel consumption [42]. Since drivers in general do not make use of the full theoretical range, the utilized range r_{util} is approximated in a second step. For this purpose, the fuel tank's average filling level at the beginning of refueling SOC_{avg} is used as follows.

$$r_{util} = r * (1 - SOC_{avg})$$

In the third step, the average number of annual refueling events per vehicle is multiplied by r_{util} in order to obtain the annual mileage. While these three steps are conducted separately for each vehicle type, the overall annual mileage mi_y can be determined by applying their respective share among the fleet as a weight and averaging results for all vehicle types.

In addition to the annual mileage, time resolved refueling probability is required. Therefore, gathered data on vehicle refueling as well as data on fleet size are used. First, each recorded refueling event is assigned to one hour of the week (e.g., 10 am to 11 am on Wednesday). Then, all events are summed up for each hour of the week and divided by the fleet size of the respective month. Thus, the number of refueling events per vehicle and hour of the week are obtained. Since the data does not cover the same number of hours for each hour of the week, the results have to be adjusted by dividing by the number of respective hours recorded. For example, if the available data covered Monday 1 am of week 1 until Monday 2 am of week 2, all hours of the week would be represented equally, except for the hour between 1 am and 2 am on Mondays. In this example, the applied adjustment would require the results of this hour to be divided by 2, since it occurs twice in the data. The overall result of this step is hourly refueling probabilities per vehicle within one week as well as the maximum occurring number of refueling events per hour and vehicle $n_{hv,max}$. Additionally, hourly refueling probabilities are aggregated per weekday in order to obtain weekday refueling probabilities.

These probabilities are complemented by an evaluation of the data per each day. As a preparatory step, all days with incomplete data are either removed from the dataset (if less than 16 h of data are available) or fixed by scaling the number of respective events to fit 24 h. Subsequently, refueling events are counted for each day and divided by the respective fleet size, resulting in average refueling events per day and vehicle $n_{d,avg}$ and the maximum number of refueling events per day and vehicle $n_{dv,max}$.

Several additional parameters are then calculated or derived, which are used in subsequent steps to create demand profiles. Table 1 gives an overview of these parameters. Some of these parameters are used to assign an HRS class (according to H2Mobility [43], see Table 2) to every fleet size by comparing $n_{d,avg}$, $n_{d,max}$ and $n_{h,max}$ to the respective values of the HRS classes. This enables other parameters to be derived from this class, e.g., the maximum hydrogen throughput per hour.

These parameters serve as an input to an algorithm, generating demand profiles for given fleet sizes. This algorithm first determines the number of days n_d that are to be covered, depending on the start and end date of the simulated time frame. Then, the total number of refueling events within this time frame are calculated by multiplying n_d by

Table 1

Parameters for demand profile generation.

Parameter	Symbol	Value/Source
Number of vehicles	n_v	According to scenario
H$_2$ consumption in kg/100 km	f_s	1, assumption
Handling time in minutes	$t_{handling}$	3, assumption
Max. number of back-to-back refuelings	n_{b2b}	1, assumption
Min. waiting time between two refueling events in minutes	t_{wait}	5, assumption
Annual mileage in km	mi_y	see above
Max. number of refueling events per hour and vehicle	$n_{h,max}$	$n_{hv,max} * n_v$
Average refueling events per day	$n_{d,avg}$	$n_{dv,avg} * n_v$
Max. refueling events per day	$n_{d,max}$	$n_{dv,max} * n_v$
Number of dispensers	n_{disp}	HRS class [43]
Max. H$_2$ throughput in kg/h	$m_{h,max}$	HRS class [43]
Average H$_2$ throughput in kg/d	$m_{d,avg}$	$\frac{n_v * mi_y}{3.65} * f_s$
Max. H$_2$ throughput in kg/d	$m_{d,max}$	$\frac{m_{d,avg} * n_{d,max}}{n_{d,avg}}$
Average dispensed H$_2$ per refueling event in kg	$m_{e,avg}$	$\frac{m_{d,avg}}{n_{d,avg}}$
Min. dispensed H2 per refueling event in kg	$m_{e,min}$	2, assumption
Min. dispensed H2 per refueling event in kg	$m_{e,max}$	$\min(7, 2m_{e,avg} - m_{e,min})$

Table 2

Parameters of HRS classes according to H2Mobility [43].

Parameter	Very small	Small	Medium	Large
Number of dispensers	1	1	2	4
Allowed waiting time between two refueling events in min	20	5	5	0
Max number of refueling events per dispenser and hour	2.5	6	6	10
Number of refueling events per day (average/max)	10/20	30/38	60/75	125/180
Max. dispensed H$_2$ in kg/h	18	33.6	67.5	224
Dispensed H$_2$ in kg/d (average/max)	56/80	168/212	336/420	700/1000

$n_{d,avg}$. These events are then distributed among the months of the time frame. Equal distribution is assumed in this case, because the provided data does not indicate different driving and refueling behavior depending on the season or month of the year. Subsequently, events are distributed among the days of each month in accordance to the previously determined daily refueling probability. Finally, all days of each month are taken into account sequentially, and events are assigned based on the hourly refueling probability. The algorithm ensures that all previously defined boundary conditions, e.g., maximum number of refueling events per hour, are met. This process is carried out in one minute resolution in order to obtain realistic profiles, avoiding refueling event collision and accounting for waiting and handling times. Due to the algorithm distributing events in a stochastic manner, the resulting demand profile does not show repetitive patterns. The demand profile is provided in hourly resolution for one year.

3.2. Modeling refueling behavior and deriving demand profiles of private vehicles

Refueling behavior of private vehicle owners in Germany is modeled according to current refueling behavior with conventional vehicles. There are no current data on refueling behavior publicly available. Instead, data on two refueling stations are used. These data are available in hourly resolution for two weeks and include volumes of gasoline and diesel fuel (passenger cars only) dispensed (see Fig. 1).

In a first step, the volumes are translated into relative refueling probabilities for every hour of one week. This can be obtained by adding the data of all four weeks (two stations with data on two weeks each) and dividing the volume of each hour by the sum of all dispensed fuel within one week. This is conducted separately for gasoline and diesel fuel. These data are merged by weighting their respective hourly probability with the respective share of gasoline and diesel vehicles among the vehicle fleet. In addition to this hourly refueling behavior within one week, seasonal refueling probabilities are determined based on monthly fuel sales. This data was gathered for the years 2012 to 2015 [44]. Only data on gasoline are used, because diesel sales are not reported separately for passenger and heavy duty vehicles. For each of these years, monthly sales are divided by total sales in the respective year and the number of days of the respective month. Results are then averaged among all years. Thus, the resulting seasonal probability reflects different behavior at the respective time of the year excluding the effect of different numbers of days per month.

The aforementioned algorithm for demand profile generation is applied, which now uses these probabilities of private refueling behavior. It stochastically allocates refueling events to points in time of one year in minute-resolution. Besides the above-mentioned data, boundary conditions of refueling station classes, defined by H2 Mobility [43], are taken into account. For this investigation, data of HRS class "very small" are used (see Table 2), because this class is the smallest available and fits the relatively low overall hydrogen demand in the current phase of infrastructure deployment. Although the algorithm distributes refueling events stochastically, it complies with these boundary condi-

tions (e.g., the maximum mass of hydrogen dispensed per day is not exceeded). The resulting demand profile is provided in hourly resolution. Its daily average hydrogen mass dispensed amounts to 53 kg/d instead of 56 kg/d due to the stochastic algorithm.

3.3. Optimizing HRS topology

The aim of topology optimization in this context is to find the best configuration of the HRS components. This comprises in some cases the dimensioning or sizing (e.g., the rated power of the electrolyzer) and in other cases, when only discrete steps of variation are possible, the number of units (e.g., compressors). These parameters can be considered decision variables of optimization. In this analysis, the quality criterion of a configuration is the levelized cost of hydrogen ($LCOH_2$) at which it can provide hydrogen. The lower the $LCOH_2$, the higher is the configuration's quality.

In this study, an evolutionary algorithm is chosen for optimization, using the main concepts of evolution: selection, recombination, and mutation [45]. In general, it approximates the best configuration stepwise. First, decision variables are defined (e.g., number of compressors and storage tank's volume) as well as respective ranges of values which they can assume. Then, several configurations, called individuals, are generated randomly by assigning each decision variable a value within the respective range. The individuals incorporate a so-called generation. All individuals are then evaluated, which means their quality is determined. Afterwards, the best individuals are selected, and new individuals are derived from them by combining the decision variable values of two individuals at a time. This process is called recombination. The third concept of evolution, mutation, is implemented by randomly altering some of the decision variables of randomly selected new individuals. The set of new individuals incorporates the second generation. They are evaluated as well, and the process is repeated until the results are considered to be close enough to optimality. The convergence criterion is a minimum number of generations (20).

Evaluation is conducted by simulating HRS operation for one year with the help of a detailed simulation model. It comprises sub-models of an alkaline electrolyzer, a low pressure storage tank, one or more hydrogen compressors, a high pressure storage, and one or more dispensers including pre-cooling (see Fig. 2). Additionally, sub-models for hydrogen demand, electricity spot market participation, and a wind farm are included. The sub-models are allowed to be non-linear, which is the case for the electrolyzer. The wind farm model is based on measured data of an existing wind farm in one-minute-resolution for one year [46]. The spot market model uses intraday prices of the year 2015, which are scaled to fit the price average of January 2017 until end of June 2017 [47]. It is assumed that the refueling station taking part in the market does not influence energy prices (price-taker approach). This might become invalid if a very large number of HRS takes part in the spot market in the future. Hydrogen demand comprises, depending on scenario, demand from carsharing fleets and private demand. The latter is modeled stochastically and based on the definition of HRS class "very small" as well as data on private refueling
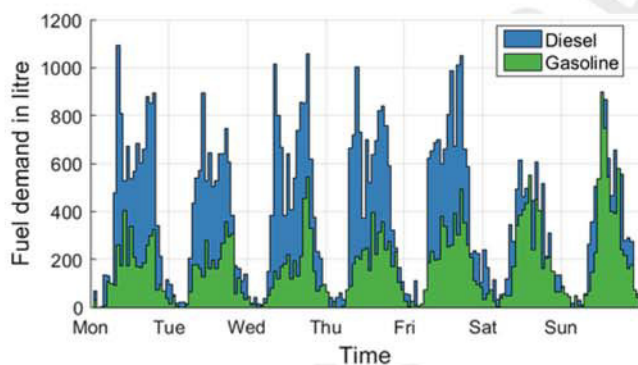

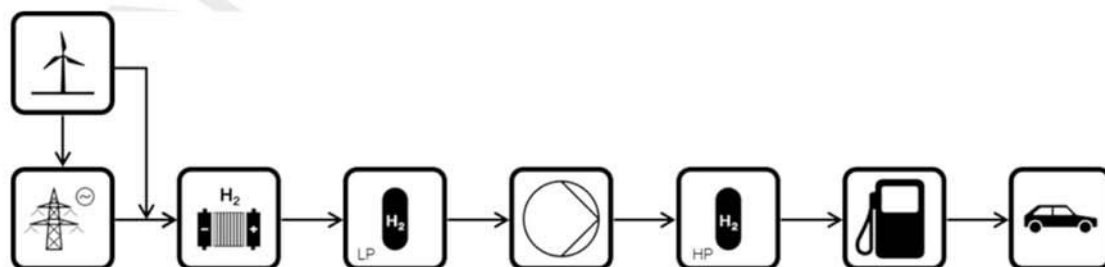**Fig. 1.** Fuel demand of two highway refueling stations.

Fig. 2. Schematic diagram of the HRS simulation model.

behavior of conventional vehicles [39]. The dispenser's pre-cooling unit is assumed to consume 0.3 kWh electrical energy per kg of dispensed hydrogen while having a stand-by demand of 2.25 kW [48]. The high pressure storage tank is not designed for providing long-term storage capabilities but as a buffer during the refueling process. Its capacity amounts to 43 kg at 1000 bar. Simulation is conducted in hourly time steps over one year. The operating strategy is rule-based and requires the electrolyzer to primarily use the wind farm's energy, and to draw energy from the grid only if the low pressure storage tank's pressure level drops below a threshold pressure. This simulation framework uses linearization and adapted linear equation system optimization per each section [49]. It has already been presented in detail [39], while the sub-models were developed in the course of a project at an existing HRS in Berlin, Germany and are described in the final project report [50].

4. Application to real-world scenarios

The presented methodology is applicable to any country or scenario. Since data is available for Germany, it is applied to this country in the following. In Section 4.1 three scenarios are defined, while cost assumptions are presented in detail in Section 4.2.

4.1. Scenarios

In this analysis, three scenarios are considered. All scenarios share the general setup of the HRS described above. The electrolyzer can draw energy from the electricity spot market and the connected wind farm. If the wind farm provides more power than the electrolyzer can consume, surplus energy can be sold at the spot market. All other components rely on the spot market only, since it must be ensured that operation is possible at any given point in time. Decision variables of optimization are depicted in Table 3. The electrolyzer's rated power is chosen according to an existing electrolyzer with 454 kW rated power at an HRS in Berlin, Germany. The lower end of this decision variable's range corresponds to 40% of this electrolyzer's rated power, and the step size amounts to 20%, accordingly. While the station's operating strategy generally is based on rules, it is also influenced by topology optimization via the decision variable "threshold pressure". If the low pressure storage tank's pressure is higher than the threshold pressure, only electric energy from the wind farm can be used, and spot market participation is prohibited. This mechanism ensures that grid electricity is only used if necessary, i.e. the storage tank's SOC is so low that proper station operation might be at stake otherwise.

The number of dispensers is not varied during optimization but determined beforehand based on the demand profile. The average daily demand is compared to the average demand of HRS classifications defined by H2Mobility [43]. The number of dispensers then is chosen according to the respective HRS class. It is assumed that only one pre-cooling unit is sufficient for any configuration. The target of optimization is to achieve configurations with the lowest possible levelized cost of hydrogen (LCOH$_2$) in €/kg. It is determined by summing up the Equivalent Annual Cost (EAC) of all components and dividing the sum

Table 3
Decision variables of optimization.

Decision variable	Range	Step size
Wind farm's rated power	0–9000 kW	100 kW
Electrolyzer's rated power	182–4086 kW	91 kW
Volume of low pressure storage tank	20–860 m^3	20 m^3
Threshold pressure	10–30 bar	5 bar

by the amount of produced hydrogen. The EAC of a component can be calculated based on the Capital Recovery Factor (CRF), the discount rate r, the life span t, the capital expenditures (Capex), the fixed operational expenditures (Opex$_{fix}$) and the variable operational expenditures (Opex$_{var}$) according to the following equations.

$$EAC = Capex * CRF + Opex_{fix} + Opex_{var}$$

$$CRF = \frac{r * (1 + r)^t}{(1 + r)^t - 1}$$

All scenarios comprise hydrogen demand from carsharing fleets. The following fleet sizes are taken into account: 10, 20, 50, 100, and 200 vehicles. In scenario 3, private demand is taken into account additionally. So the HRS configuration has to be capable of supplying not only the carsharing fleet but also private customers. It is assumed, though, that in the current initial phase of hydrogen infrastructure build-up, private demand is missing. So the HRS has to be ready to serve private demand as soon as it occurs, but earnings from selling hydrogen to these customers are missing. The capacity that has to be provided additionally for private cars is assumed to amount to 53 kg per day, corresponding to HRS class "very small" [43]. Scenario 2 is a mixture of scenarios 1 and 3, since only 25% of private demand (very small) is required to be served in addition to the carsharing fleets. But the minimum HRS size is required to have a capacity of at least 53 kg per day (serving both fleets and private cars).

4.2. Cost assumptions

For each component, Capex, Opex$_{fix}$ as well as Opex$_{var}$ are considered. Cost data are derived by evaluating several literature sources and do not include potential cost reductions in the future. Exchange rates [51] and price increases [52] are applied to Capex and Opex$_{fix}$. Thus, all cost information has been recalculated for the amount in € in the year 2016. Electrolyzer Capex are assumed to be dependent on its rated power, so a cost function is provided. All cost assumptions are summarized in Table 4. The assumed compressor is capable of handling 33.6 kg/h.

Furthermore, costs of planning, permitting, and installation are taken into account for all components except the wind turbine, as these costs are already included in its Capex. These additional costs are approximated via the sum of all Capex multiplied by a factor of 0.4 [63]. Opex$_{var}$ are determined in the course of simulation and include energy costs as well as taxes and surcharges on obtained energy.

5. Results

In the following, results for each aspect investigated are presented separately. In Section 5.1 refueling behavior of carsharing and private vehicles is analyzed and resulting demand profiles are presented. The topology optimization affects hydrogen production costs as well as ideal HRS configurations. These results are presented and discussed for each scenario in Section 5.2.

5.1. Refueling behavior and demand profiles

Regarding carsharing vehicles, the maximum number of refueling events per hour and vehicle amounts to 0.016. On average, 0.165 refueling events take place per day and vehicle, while the maximum number of refueling events per day and vehicle is 0.204. The derived refueling behavior can be expressed as relative refueling probabilities for

Table 4
Cost assumptions.

Component	Capex	Opex$_{fix}$	Life span	Source
Electrolyzer, P: power in kW	3013 € * (P/kW)$^{0.885}$	60 €/(kW*a)	20 a	[53–55]
Storage (50 bar)	632 €/kg	6 €/(kg*a)	30 a	[56,48,57,58]
Storage (1000 bar)	1144 €/kg	11 €/(kg*a)	20 a	
Compressor	394,398 €	19,720 €/a	20 a	[58–60]
Dispenser	107,000 €	5350 €/a	20 a	[58,59]
Pre-Cooling	140,000 €	7000 €/a	20 a	[58,61]
Wind turbine	1547 €/kW	56 €/(kW*a)	20 a	[62]

each hour of one week (see Fig. 3). Probabilities turn out to be very similar for weekdays from Monday to Thursday, so they are not shown and discussed separately. Moreover, Fridays are almost identical as well, but only until 2 pm (blue line vs. red line). Beyond this point in time, the number of refueling events is generally higher on Fridays. The difference is reduced during night hours and reaches zero at the overall minimum of refueling events between 4 am and 5 am. Except for a first peak between 9 am and 10 am, the number of refueling events per hour on weekdays rises monotonically until the maximum at 9 pm. Refueling behavior differs on weekends (green and purple line). The minimum is only slightly delayed and occurs between 5 am and 6 am, and the ramp up of refueling events per hour is steeper and reaches its maximum earlier at 3 pm. On Saturdays there is a plateau until 9 pm, while on Sundays the number of refueling events starts to decline at 6 pm.

On average, the annual distance traveled amounts to 19,720 km per vehicle. Derived demand profiles for different fleet sizes differ accordingly. They are not scaled based on one profile (e.g., for one vehicle) but generated stochastically. Hourly demand profiles for one exemplary week and fleet sizes of 50 and 100 vehicles are depicted in Fig. 4 and Fig. 5, respectively.

Private refueling behavior differs significantly from carsharing refueling throughout the week. It is depicted in Fig. 6. In general, there is only little refueling between 9 pm and 5 am on all days of the week. Similar to the carsharing refueling behavior, there is a rise in refueling events at about 6 am, but in contrast, it is more rapid for private vehicles. A further similarity is the delayed rise in refueling events on weekends. There is a plateau for weekdays with an evening peak at 5 pm followed by a rather sharp decline until 9 pm. On Sundays, there is a significant peak between 12 noon and 1 pm, while Saturday's profile is similar to weekdays. Overall, the modeled profile of private vehicles is less coherent and more fluctuating. This might be due to the limited time frame of data acquisition and number of refueling stations surveyed.
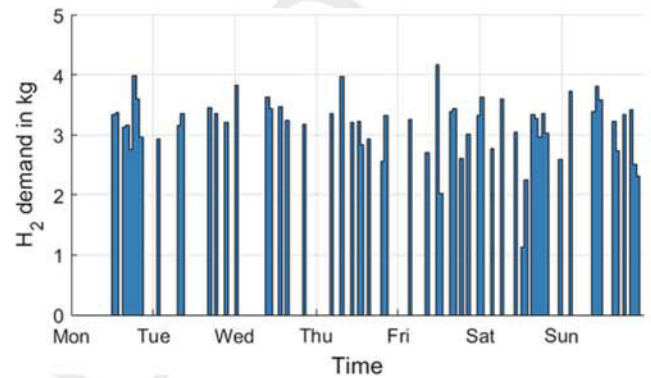

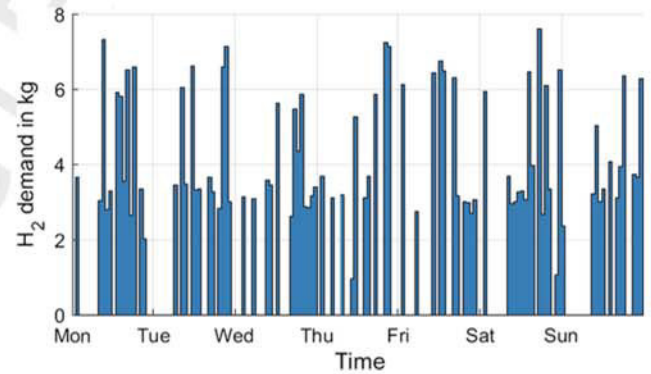Fig. 4. Exemplary demand profile of 50 carsharing vehicles.

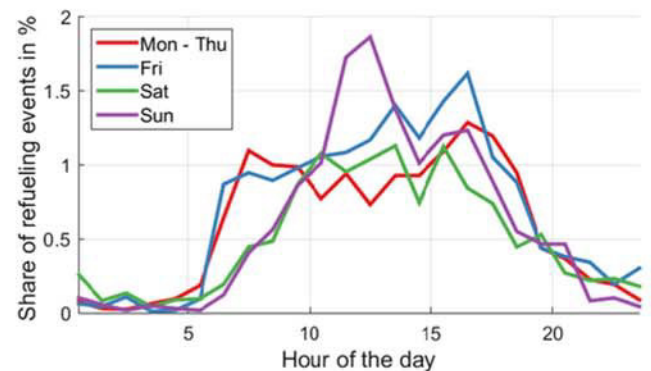Fig. 5. Exemplary demand profile of 100 carsharing vehicles.

Fig. 6. Relative probabilities of refueling events (private vehicles) within one week (averaged for Monday to Thursday).
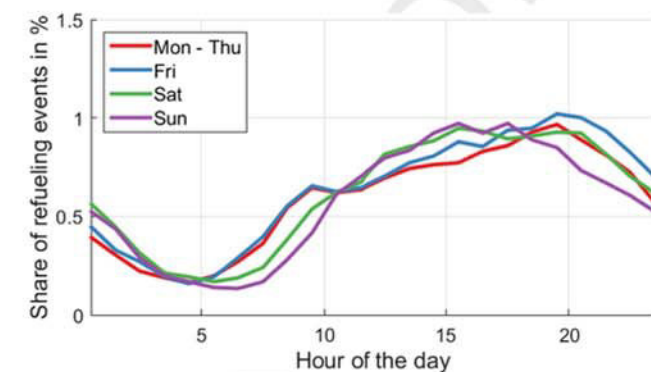

Fig. 3. Relative probabilities of refueling events (carsharing vehicles) within one week (averaged for Monday to Thursday).

In contrast to the approach dealing with carsharing refueling, private refueling behavior is modeled with the help of seasonal profiles. The distribution of refueling events among the months is shown in Fig. 7. The depicted values exclude the effect of different numbers of days
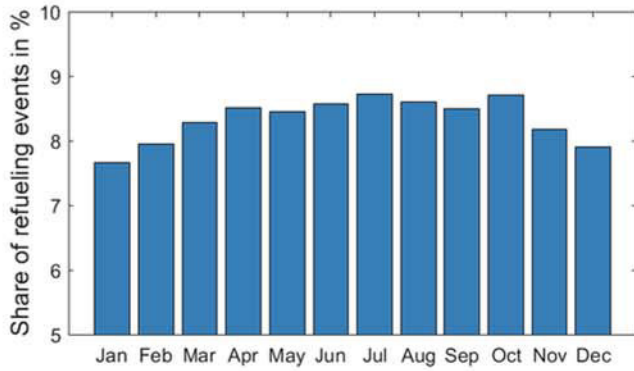
Fig. 7. Seasonal refueling probability.

per month. Between November and March, there are less refueling events per month than during the rest of the year. July and October show the most refueling events. An hourly demand profile is depicted in Fig. 8.

5.2. Topology optimization

All three scenarios are compared in terms of $LCOH_2$ in Fig. 9. For the sake of better readability and comparability, Fig. 10 shows a selection of configurations. Scenarios are differentiated by the amount of private hydrogen demand, with which the HRS has to be able to cope with in addition to the demand of fleets. There are three scenarios with five fleet sizes each, and the results of these configurations are used as sampling points (depicted as gray circles). All other values are calcu-
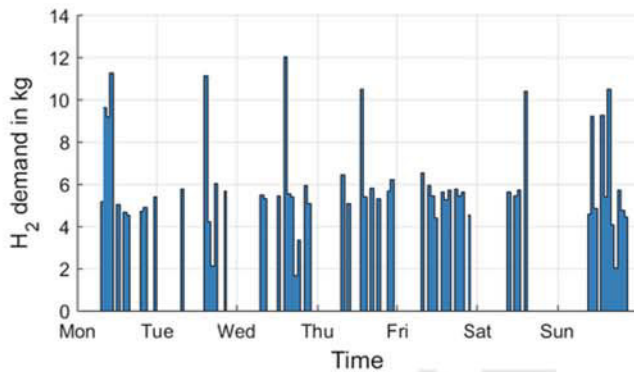
Fig. 8. Exemplary demand profile of private vehicles.
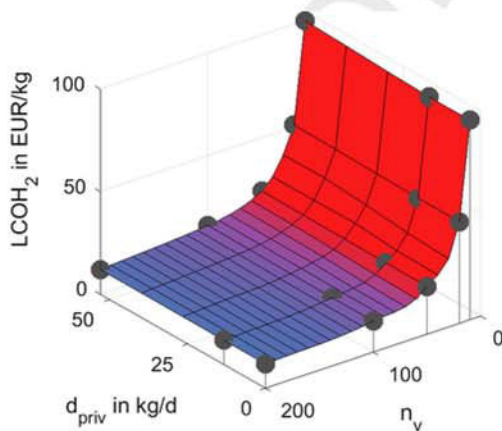
Fig. 9. Levelized cost of hydrogen ($LCOH_2$) for combinations of private demand (d_{priv}) and number of fleet vehicles (n_v). Private demand does not occur, but respective HRS capacity is required.
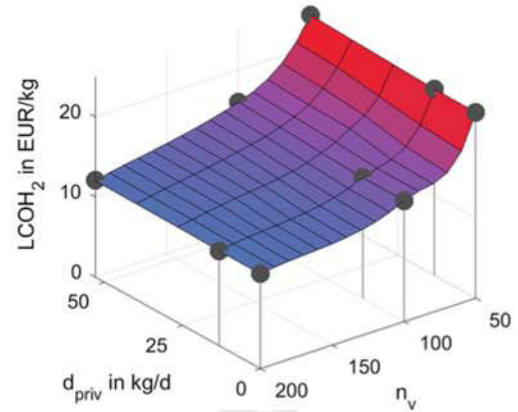

Fig. 10. Levelized cost of hydrogen ($LCOH_2$) for combinations of private demand (d_{priv}) and number of fleet vehicles (n_v). Private demand does not occur, but respective HRS capacity is required. This figure depicts a section of Fig. 9.

lated via cubic interpolation. $LCOH_2$ of cases with small fleets are very high in relation to $LCOH_2$ of larger fleets. They are also high compared to the current price that hydrogen is sold at in Germany of 7.98 €/kg (plus tax) [64]. For example, fleets of 10 and 20 vehicles result in $LCOH_2$ of about 80 €/kg and 50 €/kg, respectively. Increasing fleet size leads to significantly lower $LCOH_2$ of about 15 €/kg in case of 100 vehicles and 11 €/kg if 200 vehicles are utilized.

When relaxing the boundary condition of oversizing the HRS for private vehicles, $LCOH_2$ can be reduced. For example in case of 50 vehicles, $LCOH_2$ can be reduced from 23.94 €/kg by 3% to 23.24 €/kg if the additional capacity is lowered to 13 kg/d and to 23.21 €/kg if no additional capacity is required at all (see Fig. 10). None of the combinations reaches the market price of hydrogen.

All scenarios require the HRS to be designed to also be capable of serving private demand to a certain extent (except scenario 1), but in the current phase of HRS deployment, it is assumed that private demand has a negligible effecton revenue. Nevertheless, the HRS capacity must be sufficient for dealing with private demand if it arises in the future. Fig. 11 reveals how $LCOH_2$ is affected if private demand actually does occur in the future. Results of scenario 1 are identical, since no private demand is assumed at all – in terms of neither capacity nor actual refueling. All other scenarios benefit, and $LCOH_2$ is reduced. For example, scenario 3 (53 kg/d private demand) with 100 carsharing vehicles leads to 12.73 €/kg instead of 15.98 €/kg (−20%). Moreover, even if private demand is present, fleets can reduce $LCOH_2$ significantly, e.g., from 14.44 €/kg (50 vehicles) to 11.21 m€/kg (200 vehi-
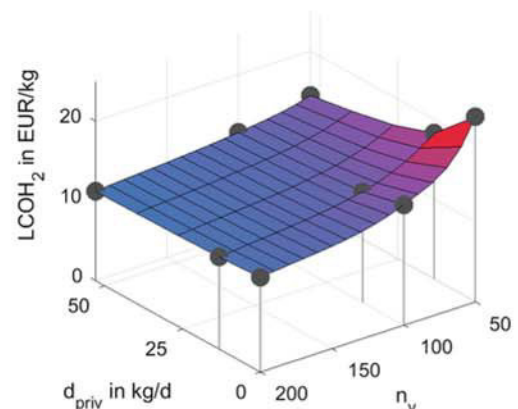

Fig. 11. Levelized cost of hydrogen ($LCOH_2$) combinations of private demand (d_{priv}) and number of fleet vehicles (n_v). Private demand is assumed to occur.

cles) in scenario 3. Nevertheless, $LCOH_2$ does not drop below 10 €/kg in any case.

In the following, only the case of missing private demand is discussed. Nevertheless, in these cases the HRS's capacity is required to also be sufficient in case private demand arises in the future. The following figures depict the decision variables of all configurations. Results of evaluated configurations are used as sampling points (depicted as gray circles). The rated power of the electrolyzer (P_{Ely}, see Fig. 12) increases with fleet size as well as private demand. There is a plateau for small fleets or low private demand due to the minimum rated power allowed. Thus, in most of these cases, the electrolyzer can be regarded oversized. The rated power of the wind turbine (P_{WT}, see Fig. 13), however, only increases with fleet size but is constant for different amounts of additional private demand. This is due to the wind turbine not being necessary, since its energy provision can be substituted by grid energy. Thus, in some cases (fleet demand rising), its rated power is increased while in other cases (private demand rising), it remains unchanged. The reason is that the wind turbine can reduce electricity costs only if adapted to the actual demand. The depicted private demand is assumed to not actually occur and lead to revenue, but only induce additional HRS capacity to cope with possible private demand in the future. Thus, the wind turbine's rated power only is adjusted to fit fleet demand.

The volume of the low-pressure storage tank (V_{LPS}) in general smoothly increases with fleet size and private demand (see Fig. 14). One exception is scenario 3 (private demand of 53 kg/d) with 50 carsharing vehicles, which shows a sharp increase compared to the same scenario with 20 fleet vehicles (60 m³ vs. 40 m³). This is due to the allowed step size of 20 m³. Thus, it can be assumed that the low-pressure
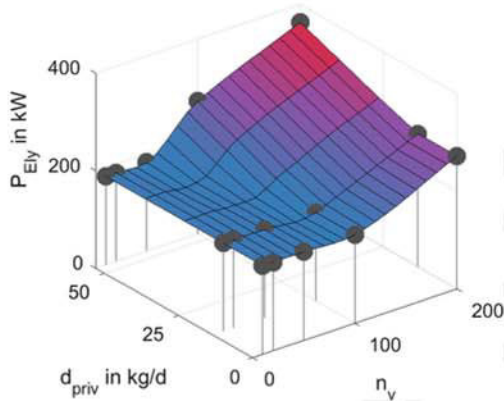

Fig. 14. Volume of the low-pressure storage tank (V_{LPS}) for combinations of private demand (d_{priv}) and number of fleet vehicles (n_v).

storage is oversized in the case of 50 vehicles. As a result, the respective electrolyzer power is not increased and thereby complements the larger storage tank volume. Moreover, it can be noticed that storage tank volume has to be adjusted even in cases of an oversized electrolyzer. The threshold pressure (p_{thres}) shows volatile behavior (see Fig. 15), indicating that it is adjusted individually to every configuration.

6. Summary, conclusion and outlook

Fuel cell vehicles using hydrogen as a fuel and carsharing are two means to cope with pollution and noise in cities. Their full potential unfolds when both concepts are combined. One major challenge is to provide a suitable refueling infrastructure for hydrogen carsharing fleets. Until now it has been unclear how such refueling infrastructure, i.e. hydrogen refueling stations, has to be designed and which costs are associated with infrastructure build-up. The paper at hand provides data on refueling behavior of conventional carsharing and private car drivers. Moreover, a methodology for deriving hydrogen demand profiles as well as for topology optimization of hydrogen refueling stations was presented. Topology optimization is based on a detailed HRS simulation model comprising onsite electrolysis and wind turbine connection. Simulations were conducted for one year in hourly resolution.

These methodologies were applied to three scenarios comprising five cases of different fleet sizes (10 to 200 vehicles) each. Thus, in total 15 setups were evaluated. Scenarios differ in a boundary condition for topology optimization, which requires the station's capacity to be capable of additionally serving private hydrogen demand. The amount

Fig. 12. Rated power of the electrolyzer (P_{Ely}) for combinations of private demand (d_{priv}) and number of fleet vehicles (n_v).
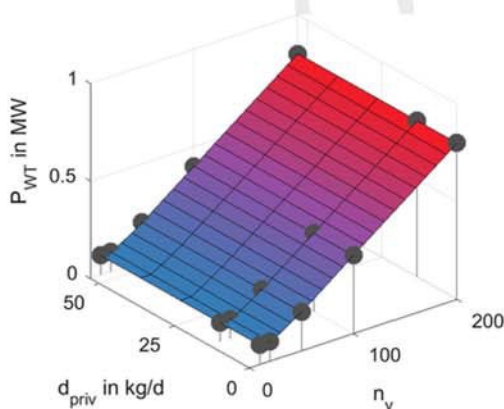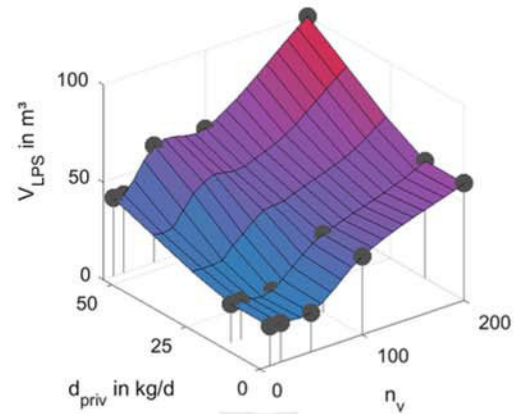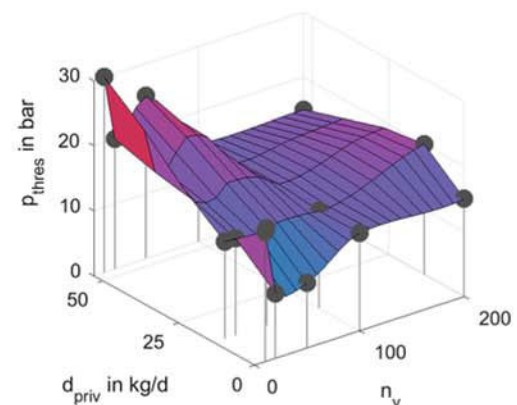

Fig. 13. Rated power of the wind turbine (P_{WT}) for combinations of private demand (d_{priv}) and number of fleet vehicles (n_v).

Fig. 15. Threshold pressure of the low pressure storage tank (p_{thres}) for combinations of private demand (d_{priv}) and number of fleet vehicles (n_v).

9

of private demand ranges from 0 kg/d (scenario 1) to 13 kg/d (scenario 2), and up to 53 kg/d (scenario 3).

Results show that the relative frequency of refueling events differs significantly during the course of one day. Furthermore, Saturdays and Sundays exhibit different refueling event distribution compared to other weekdays. Thus, refueling behavior has to be taken into account when sizing HRS to serve carsharing vehicles in order to obtain technically feasible and most cost efficient configurations. Different fleet sizes require individually adjusted HRS topology in order to achieve the lowest possible $LCOH_2$. The minimum electrolyzer power allowed in this optimization are oversized for smaller fleets. It ranges from 182 kW (10 vehicles) to 272 kW (200 vehicles). Wind turbine power varies from 100 kW to 800 kW. Low-pressure storage tank volume ranges from 20 m^3 (allowed minimum) to 60 m^3. $LCOH_2$ proves to be very high for small fleets, since some components are oversized due to minimum allowed dimensions and the electrolyzer's specific costs being high in case of relatively low rated power. Fleets of 10 vehicles induce $LCOH_2$ of about 97 €/kg, while increasing fleet size can reduce costs significantly, e.g., to 23 €/kg in case of 50 vehicles and 12 €/kg for 200 vehicles. However, costs are still high compared to the price of 7.98 €/kg at which hydrogen is currently sold at in Germany. This gap might be overcome by cost reductions in the future.

When requiring the HRS to also provide capacity for future private demand (scenarios 2 and 3), costs slightly increase. For example in case of 50 carsharing vehicles $LCOH_2$ increase by 3% (scenarios 2 and 3). The additionally required capacity affects electrolyzer and storage tank sizing but not the wind turbine, since its rated power is optimized to fit the actually occurring demand, and it can be supplemented by the electrical grid in case of additionally required electric energy.

Overall, this analysis provides important insights into infrastructure requirements for carsharing with fuel cell vehicles and its associated costs. It quantifies the relation between fleet size and hydrogen production cost. It can be concluded, that costs have to be further decreased to facilitate economically viable HRS operation for carsharing vehicles. Furthermore, oversizing of HRS for carsharing fleets in order to also serve private vehicles in the future is simulated, and costs are determined.

Future research could improve data and subsequent evaluation of refueling behavior of private drivers, since this analysis is based on only two profiles comprising two weeks each. Furthermore, centralized hydrogen production and delivery via trailer can be included in the model. Investigating spatial requirements of HRS siting and implementing a location model would add further value to this analysis.

Acknowledgment

References

[1] M. Robinius, A. Otto, P. Heuser, L. Welder, S. Konstantinos, D. Ryberg, et al., Linking the power and transport sectors - Part1: The principle of sector coupling, Energies (2017) 956.

[2] Federal Ministry of Transport, Building and Urban Development. The Mobility and Fuels Strategy of the German Government. Berlin, 2013.

[3] Agora Verkehrswende. Mit der Verkehrswende die Mobilität von morgen sichern. 12 Thesen zur Verkehrswende. Berlin, 2017.

[4] Bundesverband Carsharing e.V., Datenblatt CarSharing in Deutschland; 2018.

[5] Federal Ministry of Transport and Digital Infrastructure. Verkehr in Zahlen 2017/2018; 2017.

[6] S. Shayegan, P. Pearson, D. Hart, Hydrogen for buses in London: A scenario analysis of changes over time in refuelling infrastructure costs, Int J Hydrogen Energy (2009) 8415–8427.

[7] E. Talpacci, M. Reuß, T. Grube, P. Cilibrizzi, R. Gunnella, M. Robinius, D. Stolten, Effect of cascade storage system topology on the cooling energy consmption in fueling stations for hydrogen vehicles, Int J Hydrogen Energy 3 (2018) 6256–6565.

[8] M. Asadnia, M. Mehrpooya, Large-scale liquid hydrogen production methods and approaches: A review, Appl Energy 212 (2018) 57–83.

[9] A. Fikrt, R. Brehmer, V.-O. Milella, K. Müller, A. Bösmann, P. Preuster, et al., Dynamic power supply by hydrogen bound to a liquid organic hydrogen carrier, Appl Energy 194 (2017) 1–8.

[10] M. Eypasch, M. Schimpe, A. Kanwar, T. Hartmann, S. Herzog, T. Frank, et al., Model-based techno-economic evaluation of an electricity storage system based on Liquid Organic Hydrogen Carriers, Appl Energy 185 (2017) 320–330.

[11] H2 Mobility, Website. [Online]. Available: https://h2.live. [Accessed 28 May 2018].

[12] O. Ehret, K. Bonhoff, Hydrogen as a fuel and energy storage: Success factors for the German Energiewende, Int J Hydrogen Energy 40 (15) (2015) 5526–5533.

[13] M. Thema, M. Sterner, T. Lenck, P. Götz, Necessity and impact of power-to-gas on energy transition in Germany, Energy Procedia 99 (2016) 392–400.

[14] S. Schiebahn, T. Grube, M. Robinius, V. Tietze, B. Kumar, D. Stolten, et al., Power to gas: Technological overview, system analysis and economic assessment for a case study in Germany, Int J Hydrogen Energy (2015) 4285–4294.

[15] G. Guandalini, M. Robinius, T. Grube, S. Campanari, D. Stolten, Long-term power-to-gas potential from wind and solar power: A country analysis for Italy, Int J Hydrogen Energy (2017) 13389–13406.

[16] M. Robinius, A. Otto, S. Konstantinos, D. Ryberg, P. Heuser, L. Welder, et al., Linking the power and transport sectors - Part 2: Modelling a sector coupling scenario for Germany, Energies (2017) 957.

[17] M. McPherson, N. Johnson, M. Strubegger, The role of electricity storage and hydrogen technologies in enabling global low-carbon energy transitions, Appl Energy 216 (2018) 649–661.

[18] M. Beccali, S. Brunone, P. Finocchiaro, J. Galletto, Method for size optimisation of large wind–hydrogen systems with high penetration on power grids, Appl Energy 102 (2013) 534–544.

[19] D. Kroniger, R. Madlener, Hydrogen storage for wind parks: A real options evaluation for an optimal investment in more flexibility, Appl Energy 136 (2014) 931–946.

[20] M. Khan, M. Iqbal, Analysis of a small wind-hydrogen stand-alone hybrid energy system, Appl Energy 86 (11) (2009) 2429–2442.

[21] M. Reuß, T. Grube, M. Robinius, P. Preuster, P. Wasserscheid, D. Stolten, Seasonal storage and alternative carriers: A flexible hydrogen supply chain model, Appl Energy 200 (2017) 290–302.

[22] K. Kavadias, D. Apostolou, J. Kaldellis, Modelling and optimisation of a hydrogen-based energy storage system in an autonomous electrical network, Appl Energy, 2017, in press

[23] K. Farhat, S. Reichelstein, Economic value of flexible hydrogen-based polygeneration energy systems, Appl Energy 164 (2016) 857–870.

[24] F. Alavi, E. Park Lee, N. van de Wouw, B. De Schutter und, Z. Lukszo, Fuel cell cars in a microgrid for synergies between hydrogen and electricity networks, Appl Energy 192 (2017) 296–304.

[25] G. Kyriakarakos, A.I. Dounis, S. Rozakis, K.G. Arvanitis, G. Papadakis, Polygeneration microgrids: A viable solution in remote areas for supplying power, potable water and hydrogen as transportation fuel, Appl Energy 88 (12) (2011) 4517–4526.

[26] A. Kriston, T. Szabo, G. Inzelt, The marriage of car sharing and hydrogen economy: A possible solution to the main problems of urban living, Int J Hydrogen Energy 35 (23) (2010) 12697–12708.

[27] Linde sets up BeeZero for car-sharing in Munich. Fuel Cells Bulletin 2016;no. 4:p. 1.

[28] In brief. Fuel Cells Bulletin 2017;no. 10:p. 5–100.

[29] Clevershuttle. Press release: Mit CleverShuttle umweltfreundlich und komfortabel; 2018.

[30] S. Schmöller, S. Weikl, J. Müller, K. Bogenberger, Empirical analysis of free-floating carsharing usage: The Munich and Berlin case, Transport Res Part C: Emerg Technol 56 (2015) 34–51.

[31] M.M. Lopes, L. Martinez, G.H. de Almeida Correia, Simulating carsharing operations through agent-based modelling: An application to the city of Lisbon Portugal, Transport Res Procedia 3 (2014) 828–837.

[32] Civity Management Consultants GmbH Co. KG, Matter No. 1 - Urbane Mobilität im Umbruch? 2014.

[33] E. Troncoso, N. Lapeña-Rey, M. Gonzalez, Design tool for offgrid hydrogen refuelling systems for aerospace applications, Appl Energy 163 (2016) 476–487.

[34] S. Nistor, S. Dave, Z. Fan, M. Sooriyabandara, Technical and economic analysis of hydrogen refuelling, Appl Energy 167 (2016) 211–220.

[35] S. Carr, F. Zhang, F. Liu, Z. Du, J. Maddy, Optimal operation of a hydrogen refuelling station combined with wind power in the electricity market, Int J Hydrogen Energy 41 (46) (2016) 21057–21066.

[36] L. Zhao, J. Brouwer, Dynamic operation and feasibility study of a self-sustainable hydrogen fueling station using renewable energy sources, Int J Hydrogen Energy 40 (10) (2015) 3822–3837.

[37] J. García Clúa, R. Mantz, H. De Battista, Evaluation of hydrogen production capabilities of a grid-assisted wind–H2 system, Appl Energy 88 (5) (2011) 1857–1863.

[38] F. Grüger, F. Möhrke, M. Robinius, D. Stolten, Early power to gas applications: Reducing wind farm forecast errors and providing secondary control reserve, Appl Energy 192 (2017) 551–562.

[39] F. Grüger, O. Hoch, J. Hartmann, M. Robinius, D. Stolten, Optimized electrolyzer operation: employing forecasts of wind energy availability, hydrogen demand, and electricity prices, Eur Fuel Cell Conf 2017 (2017).

[40] K. Reddi, A. Elgowainy, N. Rustagi, E. Gupta, Impact of hydrogen refueling configurations and market parameters on the refueling cost of hydrogen, Int J Hydrogen Energy 42 (34) (2017) 21855–21865.

[41] B. Li, R. Roche, A. Miraoui, Microgrid sizing with combined evolutionary algorithm and MILP unit commitment, Appl Energy 188 (2017) 547–562.

[42] Spritmonitor.de. 2017. [Online]. Available: spritmonitor.de. [Accessed 1 12 2017].

[43] H2 Mobility. 70 MPa Hydrogen Refuelling Station Standardization - Functional Description of Station Modules; 2010.

[44] Bundesamt für Wirtschaft und Ausfuhrkontrolle. Amtliche Mineralöldaten 2013 – 2015; 2016.

[45] A. Wanitschke, Evolutionary multi-objective optimization of micro grids. Energy, Science and Technology 2015. The energy conference for scientists and researchers. Book of Abstracts, EST, Energy Science Technology, International Conference & Exhibition, Karlsruhe, Germany, 20 May 2015.

[46] Overspeed GmbH, "Measured and forecast data of wind energy production".

[47] EPEX Spot SE. [Online]. Available: https://www.epexspot.com/. [Accessed 12 12 2016].

[48] A. Elgowainy, K. Reddi, Hydrogen fueling station pre-cooling analysis. Argonne National Laboratory; 2015.

[49] F. Grüger, F. Möhrke, J. Hartman, F. Schaller, An Approach for the simulation and control of microgrids under consideration of various energy forms and mass flows. In: 9th International Renewable Energy Storage Conference; 2015.

[50] Reiner Lemoine Institut gGmbH. H2BER: Entwicklung, Erprobung und Bewertung intelligenter Betriebsstrategien für die verschiedenen Komponenten und die Gesamtsteuerung der Wasserstoff-Tankstelle am Flughafen Berlin Brandenburg (BER): Abschlussbericht: 01.01.2015-31.12.2016. TIB - Leibniz-Informationszentrum Technik und Naturwissenschaften Universitätsbibliothek, Berlin, 2017.

[51] Europäische Zentralbank. Euro-Referenzkurs der EZB; 2017.

[52] Statistisches Bundesamt. Verbraucherpreisindizes für Deutschland; 2017.

[53] C. Greiner, M. Korpas, A. Holen, A Norwegian case study on the production of hydrogen from wind power, Int J Hydrogen Energy 32 (10–11) (2007) 1500–1507.

[54] T. Smolinka, M. Günther, J. Garche, Stand und Entwicklungspotenzial der Wasserelektrolyse zur Herstellung von Wasserstoff aus regenerativen Energien, Kurzfassung des Abschlussberichtes NOW-Studie (2011).

[55] C. Noack, F. Burggraf, S. Hosseiny, P. Lettenmeier, S. Kolb, S. Belz, J. Kallo, K. Friedrich , T. Pregger, Studie über die Planung einer Demonstrationsanlage zur Wasserstoff-Kraftstoffgewinnung durch Elektrolyse mit Zwischenspeicherung in Salzkavernen unter Druck; 2014.

[56] Hydrogen Delivery - Technical Team Roadmap. United States Driving Research and Innovation for Vehicle Efficiency and Energy sustainability; 2013.

[57] K. Stolzenburg, R. Hamelmann, M. Wietschel,F. Genoese, J. Michaelis, J. Lehmann, A. Miege, S. Krause, C. Sponholz, S. Donadei, Integration von Wind-Wasserstoff-Systemen in das Energiesystem. NOW-Studie, Berlin; 2014.

[58] P. Hill, M. Penev, Hydrogen fueling station in honolulu, Hawaii Feas Anal (2014).

[59] G. Parks, R. Boyd, J. Cornish, R. Remick, Hydrogen station compression, storage, and dispensing technical status and costs: Systems integration, Nat Renew Energy Lab (NREL) (2014).

[60] U. Bünger, H. Landinger, E. Pschorr-Schoberer, P. Schmidt, W. Weindorf, J. Jöhrens, et al., Power-to-Gas (PtG) im Verkehr-Aktueller, Stand und Entwicklungsperspektiven (2014).

[61] P. Dahl, U. Bünger, S. Völler, M. Korpaas, S. Moller-Holst, Hydrogen for transport from renewable energy in Mid-Norway; 2013.

[62] S. Lüers, A.-K. Wallasch, K. Rehfeldt, Kostensituation der Windenergie an Land in Deutschland - Update, Deutsche Windguard (2015).

[63] J. McKinney, E. Bond, M. Crowell, E. Odufuwa, Joint agency staff report on assembly bill 8: assessment of time and cost needed to attain 100 hydrogen refueling stations in California. California Energy Comission and California Air Resources Board; 2015.

[64] Clean Energy Partnership. Press-release: Environment Minister Franz Untersteller opened a stand-alone, hydrogen filling station in Stuttgart; 2013.